

Off-Equilibrium Dynamics of 1+1 dimensional Directed Polymer in Random Media

Hajime Yoshino

Institute of Physics, University of Tsukuba, Tsukuba, Japan

email: yoshino@cm.ph.tsukuba.ac.jp

Abstract

The relaxational dynamics of 1+1 dimensional directed polymer in random potential is studied by Monte Carlo simulations. A series of temperature quench experiments is performed changing waiting times t_w . Clear crossover from quasi-equilibrium behavior ($t \ll t_w$) to off-equilibrium behavior ($t \gg t_w$) appears in the dynamical overlap function whose scaling properties are very similar to those found in the 3 dimensional spin-glass model. In the $t \gg t_w$ part, the fluctuation dissipation theorem of the 1st kind which relates the response function to the tilt field with the conjugate correlation function, is found broken. These aging effects are brought about by the very slow growth of quasi-equilibrium domain driven by successive *loop-excitations* of various sizes, which form complex network structures.

02.50.Ey, 74.60.Ge, 75.10.Nr.

arXiv:cond-mat/9510024v2 6 Oct 1995

Typeset using REVTeX

I. INTRODUCTION

Directed polymer in random media (DPRM) [1] is one of the simplest statistical mechanical models in which quenched randomness plays non-trivial roles as in spin-glasses. It is an effective model of an elastic string in random environment, such as a vortex line in oxide cuprate superconductor which penetrates the stacked CuO_2 layers with point defects scattered randomly over the layers. In transverse dimensions d less than two, there is no *free phase* but a *pinned phase*, i.e. the polymer is mostly pinned around the ground state and cannot move freely at any finite temperature. However there are anomalously large thermal fluctuation due to the thermal hoppings between the excited states which are nearly degenerate with the ground state but located far away. They are analogous to the droplet excitations in spin-glass phase [2] and bring about non-trivial effects in the pinned phase [3–5]. One naturally expects that they have dramatic effects also on the dynamics. Actually, it has been argued in the theory of the transport problem in the vortex glass phase that they are responsible for the nonlinear current-voltage response [6].

Our interest in the present study is the slow relaxation to equilibrium due to such anomalous thermal hoppings. We expect that they bring about aging effects, which are to some extent similar to those found in the spin-glass phase. In order to clarify this possibility, we performed temperature quench experiments by a simple heatbath Monte Carlo dynamics. The procedure mimic the so called IRM experiments in spin-glasses [7] but the system is perturbed by a small *tilt* field which drives one end of the polymer instead of magnetic field in spin-glasses which drives the whole spins .

We have found clear evidences of the aging effects. One is the systematic waiting time dependence on the dynamical overlap function. The crossover behavior from quasi-equilibrium to off-equilibrium behavior and its scaling properties are, interestingly enough, very similar to that found in the spin-autocorrelation function of the 3 dimensional spin-glass model [9]. The 2nd is the break down of the fluctuation dissipation theorem (FDT) associated with the response to the tilt field. Again the correlation function which is conjugate with the

response function shows clear waiting time dependence. On the other hand, in contrast with the case of spin-glasses, the response function itself does not show waiting time dependence. The FDT which relates the two breaks down at $t \gg t_w$, which coincide with the crossover behavior in the dynamical overlap function.

In our analysis we also utilize the transfer matrix method for the following two purposes. Firstly, we check the consistency between the static limit of the data of the dynamical quantities and the static expectation values. Secondly we study the relation between the complex free energy landscape and the relaxational dynamics. Actually we could visually monitor the thermal jumps between the excited states. The structure of the web of the excited states is very complex which consists of numerous loop-like structures of various sizes (see Fig. 3 below). Since this model is rather simpler than spin-glass models, we believe that understanding the dynamics of this model would give valuable insight into the glassy dynamics of more complicated systems.

This paper is organized as the following. In section 2 we describe our model and introduce the Monte Carlo dynamics. In section 3, the elementary process of the dynamics is studied combining with the analysis of the free energy landscape by the transfer matrix method. In section 4, the procedure of the temperature quench experiment is described. The results are given in section 5. In section 6 we conclude this paper with some phenomenological arguments.

II. THE MODEL

We study a lattice version of 1+1 dimensional directed polymer in random media (DPRM). The Hamiltonian is

$$\mathcal{H}_\mu[x] = \sum_{z=1}^N \{g|x(z) - x(z+1)| + \mu(x(z), z)\} - hx(N) \quad (1)$$

where $x(z)$ ($z = 1 \cdots N$) represents the configuration of the polymer whose length is N . As shown in Fig. 1, the polymer is situated on a square lattice and *directed* along the z -axis

so that overhangs are excluded. We impose the so called restricted solid on solid (RSOS) condition, i.e. the steps $|x(z) - x(z - 1)|$ are only allowed to take integer values $-1, 0$ and 1 . We fix one end $x(0)$ at $x = 0$ while we allow the other end $x(N)$ to move freely. The 1st term in the Hamiltonian represents the elastic energy. The 2nd term represents the random potential which takes random numbers distributed uniformly over $-\sigma \leq \mu \leq \sigma$ independently on every lattice site on the square lattice. The last term is the tilt field which drives the free end and *tilts* the polymer.

We model the relaxational dynamics of the present model by an ordinary heatbath Monte Carlo dynamics as in the following way. In one micro Monte Carlo step (micro-MCS), one segment, say the segment at $z = z_0$ is tried to move. The new position is chosen among the possible choices allowed by the RSOS condition with the appropriate transition probabilities so as to satisfy the detailed balance condition. As shown in Fig. 2, this micro-MCS can be classified into three cases depending on the positions of the neighboring segments at $z_0 - 1$ and $z_0 + 1$, namely case a), b) and c) which corresponds to $|x(z_0 - 1) - x(z_0 + 1)| = 0, 1$ and 2 respectively. The entire configuration is refreshed by vectorized sublattice flippings in one Monte Carlo step (MCS) (=N micro-MCS). One sublattice consists of the even numbered segments $z = 2, 4, 6 \dots$ and the other sublattice consists of the odd numbered segments $z = 1, 3, 5 \dots$

III. ELEMENTARY PROCESSES OF THE DYNAMICS

In this section we consider the elementary processes of the relaxational dynamics in the present model. In any quenched random systems, it is generally essential to understand the structure of the free energy landscape in order to study the slow relaxational dynamics, which is unfortunately very hard to do on spin-glass models. However, thanks to the simplicity of the model, we can try such an attempt on the present model in the following way. We consider the spatial variation of $P_\mu(z, x)$: the probability to find the polymer going through a particular lattice point (z, x) on a certain sample of random potential μ . It is defined as

$$P_\mu(z, x) = Z_\mu^{-1} \sum_{\text{configuration}} \delta(x(z) - x) \delta(x(0) - 0) \exp(-\beta \mathcal{H}[x, \mu]) \quad (2)$$

where the sum is taken over the all possible configurations (or paths) $\{x(1), \dots, x(N)\}$ and Z_μ is the normalization factor defined so that $\sum_{x=-z}^z P_\mu(z, x) = 1$. It is straightforward to calculate this probability by transfer matrix method [1]. In Fig. 3, an example of the spatial variation of $P_\mu(z, x)$ of a system of $N = 100$, $T = 0.3$, $g = 0.01$ and $\sigma = 0.5$ on a certain sample of random potential μ is displayed by a density plot; the intensity increases as the color becomes brighter. We recognize that most of the probability density is confined in the white *tubes* which are understood as the thermally active excited states. In the dynamics, they presumably serve as *traps* [12], which tend to trap the polymer for long times. On the other hand there are black *voids* between the tubes which presumably serve as free energy barriers. It is quite remarkable that the tubes form a very complicated network which consists of various sizes of loop-like structures. It is qualitatively consistent with the prediction by Hwa and Fisher [4] who have predicted a broad distribution of the size of the loops. As the temperature increases, one can observe that the diameter of the tubes grows and the structure itself changes on large scales as predicted in [3].

From the above observation, we speculate that the dynamics of the polymer roughly consists of the two kinds of elementary processes. One is the fast fluctuation within each tubes (traps). The other is the thermally activated jumps between such tubes, which is analogous to the droplet excitations in spin-glasses. Actually these two different processes can be visually monitored rather easily as the following. In Fig. 4 we plot the time sequence of the segment $x(80)$ on the same system shown in Fig. 3. The data are averaged over every interval of 10^3 (MCS) trying to mask small scale fluctuations. Apart from the remanent small scale fluctuations, which is understood as the fast fluctuations within each traps (tubes), the coarsegrained process is apparently understood as jumps between the four traps which correspond to the four major peaks of $P(80, x)$ (white tubes in Fig. 3 at $z = 80$).

The thermal jumps between the traps must go over the free energy barriers which lie between them (black void in Fig. 3). The scaling property of the relaxation times of the

thermal jumps between the tubes has already been studied in the context of the aforementioned transport problem in the vortex glass phase [6]. For the convenience of the later discussions, we summarize it here. For example, suppose that there is a loop-like structure of tubes as schematically shown in Fig. 5. Let its transverse size Δ . Then the free energy barrier $F_B(\Delta)$ associated with the thermal excitation over the loop, which we hereafter call *loop-excitation* following [6], scales as

$$F_B(\Delta) \simeq a(T)\Delta^\alpha, \quad (3)$$

where $a(T)$ is some temperature dependent constant. Note that near the free end of the polymer, the tubes does not form complete loop structures but rather *U*-shaped structures in which one side of the ends of the tubes are left open. But we expect that such thermal excitations scales in the same way as the *complete* loop excitations. The value of the exponent α is expected to be 1/2 in 1+1 DPRM [4]. Then the relaxation time of the loop-excitation scales as

$$\tau(\Delta) \sim \exp(F_B(\Delta)/T) \simeq \exp\left(\frac{a(T)\Delta^\alpha}{T}\right). \quad (4)$$

The broad distribution of the size of the loops [4] implies broad distribution of relaxation times.

IV. PROCEDURE OF THE TEMPERATURE QUENCH EXPERIMENT

The numerical experiment is done in the following way (see also the illustration in Fig. 6). At first, a random initial configuration is prepared. Then the system is let to evolve for t_w (MCS) by the heatbath Monte Carlo dynamics of a certain temperature T . This means that the polymer is forced to approach the equilibrium state of temperature T being attached to a heat bath of temperature T . After this t_w (MCS) of *aging*, the polymer's configuration is stored and copied to a replica system. Then we let the two systems, say replica A and B, continue the relaxational dynamics using the same random numbers (same thermal noise of the heat bath) but applying small tilt field h to system B.

We measure the following dynamical overlap function as a probe to the relaxational dynamics of the unperturbed system (replica A). It is defined as

$$q(t_w + t, t_w) \equiv \overline{\left\langle \frac{1}{N} \sum_{z=1}^N \delta(x^{(A)}(z, t_w + t), x^{(A)}(z, t_w)) \right\rangle}, \quad (5)$$

where $\delta(x, y)$ is the Kroneker's delta and $x^{(A)}(z, t)$ ($z = 1 \dots N$) represents the configurations of the polymer at t (MCS). Here the bracket $\langle \dots \rangle$ denotes the average over different sequences of the random numbers and the over bar $\overline{\dots}$ the average over different realizations of the random potentials. It is defined in an analogy with the spin-autocorrelation function of the spin-glass models and conveniently measure the 'closeness' between the configurations at two different times $t_w + t$ and t_w . In the static limit, it is expected to converge to the expectation value of the overlap q_{rep} between two replica systems which has been introduced by Mézard [5],

$$q_{\text{rep}} = q_{\text{static}} \equiv \lim_{t \rightarrow \infty} \lim_{t_w \rightarrow \infty} q(t_w + t, t_w). \quad (6)$$

We measure the dynamical response to the tilt field at t (MCS) after t_w (MCS) of aging as the distance between the temporal positions of the free end $x(N)$ of the two replicas A and B, which we denote as $x_e^{(A)}(t_w + t)$ and $x_e^{(B)}(t_w + t)$,

$$\overline{\delta x_e(t; t_w)} \equiv \overline{\langle x_e^{(B)}(t_w + t) - x_e^{(A)}(t_w + t) \rangle}. \quad (7)$$

Note that $\langle \dots \rangle$ encloses both $x_e^{(A)}(t)$ and $x_e^{(B)}(t)$ because we use the same random numbers in replica A and B in our procedure. This definition is slightly different from the conventional one $\overline{\langle x_e^{(B)}(t_w + t) \rangle} - \overline{\langle x_e^{(A)}(t_w + t) \rangle}$. However our present choice is more efficient in practice because it provides essentially the same result but with less noise.

In equilibrium, the response function (7) is related with the correlation function

$$C_e(t_1, t_2) = \overline{\langle x_e^{(A)}(t_1) x_e^{(A)}(t_2) \rangle} \quad (8)$$

as

$$\overline{\delta x_e(t; t_w)} = h \int_{t_w}^{t_w+t} R_e(t + t_w, \hat{t}) d\hat{t} = \beta h [C_e(t_w + t, t_w + t) - C_e(t_w + t, t_w)], \quad (9)$$

by the fluctuation dissipation theorem (FDT) of the 1st kind,

$$R_e(t_1, t_2) \equiv \overline{\delta x_e(t_1 - t_2; t_2)} / \delta h(t_2) = \beta \partial C_e(t_1, t_2) / \partial t_2 \quad (10)$$

provided that h is small enough (linear response regime). Note that in the static limit $t_w \rightarrow \infty$ and $t \rightarrow \infty$ of (9), we get the ordinary static FDT,

$$\overline{\langle x_e \rangle_h} = \lim_{t \rightarrow \infty} \lim_{t_w \rightarrow \infty} \overline{\delta x_e(t_w; t)} = \beta h \chi \quad (11)$$

where the susceptibility χ is given by

$$\chi = \overline{\langle x_e^2 \rangle} - \langle x_e \rangle^2. \quad (12)$$

We performed a series of temperature quench experiments on the system with various sizes $N = 20 \dots 300$, and temperatures at $T = 0.1 \dots 0.5$. The parameter g and σ are fixed at $g = 0.01$ and $\sigma = 0.5$. The average over $10^4 \dots 10^2$ samples of random potential were done depending on the system size. In order to ensure that h is small enough so that the linear response condition is satisfied, we calculated the disorder averaged static susceptibility χ (see (12)) and $\overline{\langle x_e \rangle_h}$ by the transfer matrix method [5] and checked that (11) is well satisfied.

V. RESULT

A. Crossover Behavior of Dynamical Overlap Function

We first present the results of the dynamical overlap function defined in (5) on the unperturbed system (replica A). The following analysis is done on the data of $N = 300$ at $0.1 < T < 0.5$. The observation was done in the time window ($0 < t < 10^4$ (MCS)) for $t_w = 2, 2^2, \dots, 2^{10}$ (MCS). The data at $T = 0.1$ and 0.3 are plotted by double logarithmic plot in Fig. 7. The remarkable feature is that the data curves show strong waiting time t_w dependence and each of them drops off rapidly at around $t \sim t_w$. It is presumably understood as a manifestation of the crossover from the quasi-equilibrium behavior ($t \ll t_w$)

to the off-equilibrium behavior ($t \gg t_w$), i.e. aging effect. Actually we see later that it coincides with the FDT breaking which also occurs at around $t \sim t_w$.

The quasi-equilibrium regime ($t \ll t_w$) begins with an initial fast decay and crossovers to a much slower decay, which is only visible on the data curves of sufficiently large t_w . Unfortunately we cannot determine the asymptotic functional form ($t_w \gg 1$) of the latter slow decay at this moment. However the scaling analysis which we discuss later suggests an algebraic law (see (17) below) with very small exponent $x(T)$ which varies with the temperature as shown in Fig. 10. On the other hand, the off-equilibrium part is well fitted by an algebraic law

$$q(t_w, t_w + t) \sim t^{-\lambda(T)} \quad (t \gg t_w), \quad (13)$$

where the exponent $\lambda(T)$ also depends on temperature as shown in Fig. 10. It is interesting to note that these characteristics of the crossover behavior are very similar to those originally found by Rieger [9] in the spin-autocorrelation function of the 3 dimensional Edwards-Anderson spin-glass model in the spin-glass phase.

We now analyze the scaling properties of the dynamical overlap function. We try the scaling form

$$q(t_w, t_w + t) \simeq C(t_w, T) \tilde{q}_T(t/t_w). \quad (14)$$

As an example, the scaling plot of the data of $N = 300$, $T = 0.17$ is shown in Fig. 8. The parameter $C(t_w, T)$ was chosen so as to scale the off-equilibrium part ($t/t_w \gg 1$) as good as possible. It turns out that the initial fast decay part, which we mentioned before, does not fit on the master curve of the t/t_w scaling. In practice, we could obtain the scaling plot shown in Fig. 8 discarding the data of $t \leq 10$ (MCS). At higher temperatures we have to discard more data to obtain good master curves.

As expected, the scaling function behaves as $\tilde{q}_T(y) \sim y^{-\lambda(T)}$ at $y \gg 1$ with $\lambda(T)$ which we found in (13). On the other hand the constant $C(t_w, T)$ turns out to be well fitted by an algebraic law of t_w ,

$$C(t_w, T) \sim t_w^{x(T)}, \quad (15)$$

as shown in Fig. 9. The exponent $x(T)$ obtained by this fitting varies with temperature as presented in Fig. 10. At $T < 0.17$, $x(T)$ becomes too small to be determined precisely.

Using (15), we can rewrite (14) as

$$q(t_w, t_w + t) \simeq t^{-x(T)} \phi_T(t/t_w) \quad (16)$$

where $\phi_T(y)$ is related with $\tilde{q}_T(y)$ in (14) by $\phi_T(y) \equiv y^{x(T)} \tilde{q}_T(y)$. Note that this scaling form is also identical to that originally found in 3 dimensional spin-glass model by Rieger [9]. The new scaling form (16) implies that the quasi-equilibrium part ($t/t_w \ll 1$) behaves as

$$q(t_w, t + t_w) \sim t^{-x(T)} \quad (t_w \gg 1, \quad t/t_w \ll 1). \quad (17)$$

However as can be seen in the master curve in Fig. 8, the crossover takes place rather gradually and the left branch of the master curve ($t/t_w \ll 1$) seem to decay faster than the expected algebraic law $t^{-x(T)}$ with $x(T)$ obtained from (15). This discrepancy implies that we have not yet attained the asymptotic scaling behavior of the $t/t_w \ll 1$ part. Unfortunately we could not accomplish it with our available computational power.

Lastly we discuss the finite size effects. As far as the system size N is finite, the size of the largest loop-excitation and thus the associated maximum relaxation time $\tau_{\max}(N)$ available in the system must be finite (see (4)). Thus we expect that system is fully equilibrated if we take t_w larger than a certain equilibration time $t_{\text{eq}}(N)$ which may be comparable with the $\tau_{\max}(N)$. The finite size effect appears in the dynamical overlap function as the following. In Fig. 11 the data on the system of $N = 20$ and $T = 0.5$ is shown as a typical example. It can be seen that the waiting time t_w dependence on the dynamical overlap function saturates at some finite t_w as t_w is increased: the curves do not show any further t_w dependence when t_w exceeds some characteristic time $t_{\text{eq}}(N)$. In the example shown in Fig. 11, it is larger than 2048 but less than 16384 (MCS). We have checked that $t_{\text{eq}}(N)$ increases as we increase the system size N . It is also recognized that the dynamical overlap function saturates to the static limit q_{static} (see (6)) when $t \gg t_{\text{eq}}$. The value of q_{static} is nearly equal to q_{rep}

obtained by transfer matrix method which uses two replicas [5]. Though q_{rep} is non-zero in finite systems, further calculations by the transfer matrix method on larger systems show that q_{rep} decrease as the system size N increases and it vanish in the thermodynamic limit $N \rightarrow \infty$ (see [5]).

B. Breakdown of FDT

We next present the results of the response to the tilt field defined in (7). The curves in Fig. 12 shows the l.h.s and r.h.s. of the FDT relation (9) at different waiting times $t_w = 40, 200$ and 1000 (MCS) on the system of $N = 20$ at $T = 0.2$ with the tilt field $h = 0.1$ by semi-logarithmic plot. The quench experiment was done over 10^4 different samples of random potential in order to take sufficient average over the disorder. The curves of the l.h.s. of (9) (correlation) strongly depends on the waiting time t_w . On the other hand, the curves of the r.h.s of (9) (response) of corresponding t_w do not seem to have significant t_w dependence and almost seem to merge with each other within the numerical accuracy. Comparing with the data of larger system sizes, we checked that the data are not spoiled by finite size effects within this observation time window ($0 < t < 10^4$ (MCS)). However it is difficult to get smooth data on larger systems because they are not self-averaging quantities and sample to sample fluctuations are larger on larger systems.

As is clear from the figure, the FDT relation is satisfied in the regime $t \ll t_w$ but broken in the regime $t \gg t_w$. It is again a clear evidence of the crossover from quasi-equilibrium to off-equilibrium dynamics, i.e. aging effect. Similar FDT breaking was previously found in the spin-glass phase of the 3 dimensional spin-glass models by Monte Carlo simulations [10,11]. However there is an important difference: in the spin-glass models both the response and correlation functions strongly depends on t_w while in the present model the response dose not seem to have t_w dependence. This is understood as the following. As the tilt field pulls the free end of the polymer, it moves by successive local thermal excitations around it, while the rest of the system is indifferent of the existence of the tilt field. We expect that

the free energy barrier of such thermal excitations scales as (3). Thus the response will scale the same way as the *typical* transverse size of a loop-excitation which becomes active after waiting t ,

$$\overline{\delta x_e(t; t_w)} \sim \log(t)^{1/\alpha}. \quad (18)$$

In order to clarify this scaling form, we performed longer simulation up to 10^5 (MCS). In Fig. 13 we show the double logarithmic plot of $\overline{\delta x_e(t; 0)}$ v.s. $\log(t)$ on the system of $N = 30$, $T = 0.20$ and $N = 60$ at $T = 0.30$ with $h = 0.03$. It can be seen that the behavior is consistent with (18) with $\alpha = 1/2$ and thus supports the above argument. The data on the system of different system sizes and at different temperatures show similar behavior except that data of smaller systems show saturations within the observation time window.

Lastly we consider the extremely high temperature case in finite systems. As we mentioned before the diameter of the tubes grow as the temperature increases [4]. Then if the system is too small, a single tube swallows up the whole system and the thermal jumps between the tubes disappear. In Fig. 14 is shown an example of free energy landscape for such case, the density plot of $P_\mu(z, x)$ of a system of $N = 20$ at $T = 1.0$ on a certain random potential. Roughly only a single big tube can be recognized. In such an extreme case, we found no aging effects. The FDT relation is fulfilled in the whole t range up to the static limit as shown in Fig. 15. At around 10^3 (MCS), they saturate to the static limit, $\overline{\langle x_e \rangle}_h$ or $h/T\chi_e$ (see (11)) calculated by the transfer matrix method. In addition, the dynamical overlap function does not show any t_w dependence. These facts suggest that the thermal jumps between the tubes, i.e. loop-excitations are the essential processes to bring about the observed aging effects.

VI. CONCLUSION

The relaxational dynamics of 1+1 dimensional DPRM was investigated by the Monte Carlo simulations which mimiced the IRM experiment in spin-glasses. The aging effect

appears as the systematic waiting time dependence on both the dynamical overlap function and the FDT breaking. The dynamical overlap function shows clear crossover from slow quasi-equilibrium decay ($t \ll t_w$) to fast off-equilibrium decay ($t \gg t_w$). The latter is well fitted by an algebraic law whose exponent depends on temperature. The t/t_w scaling scheme works well and it suggests algebraic decay also in the quasi-equilibrium part. However we could not confirm the latter directly with our computational power. On the other hand, the response to the tilt field grows as $\log(t)^2$ (18) independently of the waiting time, which supports the assumed scaling properties of loop-excitations (see (3) and (4)). Concerning the fact that it does not show t_w dependence, this model appears rather trivial compared with, for example, spin-glasses in which there are dramatic effects also in the response function so that one can actually observe the aging effects in experiments by measuring the magnetization [7,8]. None the less, other aspects of the aging effect are very similar to that found in the spin-glass phase of 3 dimensional spin-glass models [9–11]. Hence we believe that this model provides a good testing ground for various theoretical ideas of the slow dynamics of quenched random systems.

The important elementary processes to bring about the observed aging effect are the loop-excitations, i.e. thermal hoppings between the traps (tubes) in the free energy landscape. They were actually demonstrated by direct monitoring of the time sequences. Thus equilibration process is understood as the slow growth of quasi-equilibrium domain driven by successive loop-excitations. Note that this growth mechanism of the quasi-equilibrium domain is essentially the same as proposed in the spin-glass models in which droplet excitations drive the growth of the domain [2]. From (4), we expect that its transverse size $R(t)$ grows as

$$R(t) \sim \log(t)^{1/\alpha}. \quad (19)$$

However the scaling properties of the dynamical overlap function are not trivial. Though they turned out to be quite similar to those found in the spin-glass model [9], they cannot be explained by simply borrowing the assumptions of the above mentioned droplet theory

[2]. In the droplet theory, it is assumed that

$$q(t, 0) \sim R(t)^{-\lambda}, \quad (20)$$

where $q(t_1, t_2)$ is now the spin-autocorrelation function and λ is some unknown exponent [2]. (Here λ is the notation of [2] and different from $\lambda(T)$ defined in (13).) But we don't have any reason to believe that such a relation exists in the present model, and actually our result (13) cannot be consistent with (19) if we assume (20). In the study of spin-glass model [9], it is argued that (13) can be consistent with (20) if one assumes that the free energy barrier grows logarithmically with its transverse size Δ rather than algebraically so that $R(t)$ grows algebraically with a certain temperature dependent exponent. If it is the also case in the present model, the response function (7) should be fitted by such algebraic law. However our data of the response function show systematic curvature in double logarithmic plots and do not prefer such algebraic law but the logarithmic law (18). Thus we conclude that the simple relation (20) does not exist in the present model. The scaling properties of the dynamical overlap function require other ways to explain them.

The important feature we recognize in Fig. 3 is that the tubes are grouped together to form some very complicated network. We already know how the relaxation time associated with each single loop-excitation scales with its transverse size (see (4)). However there is an obvious but important rule: a loop-excitation can *flip* only when some part of the temporal configuration of the polymer actually stay in either side of the loop, in other words the *empty* loops can not *flip*. It should also be noted that the polymer is *not* allowed to be broken into pieces during the dynamical process. Thus not the entire loop-excitations built in the system can become *active* simultaneously but only those which are associated with the sequence of the loops which contain the actual temporal configuration of the polymer. From the above considerations, it is clear that the information of the connectivity of the loops is an important ingredient to describe the dynamics of the polymer.

Let us now consider the dynamical overlap function (5). It can be roughly interpreted as the *probability* that the segments of the polymer return to the original traps in which

they initially stay after jumping around other traps in the network. Here we need the detailed description of the dynamics mentioned above since the probability is the sum of the probabilities associated with all of the possible paths which make such return trips. Each of these paths consist of different sequences of loop-excitations which vary in sizes and thus have different relaxation times. It is unlikely that there is a single *typical* mode whose probability dominate the total probability. On the other hand, the response to the tilt field does not depend directly on such details. The response function scales just as the *expectation value* of the transverse size of the local loop-excitation around the free end which can become active after waiting t . It is possible that such expectation value is dominated by the contribution from the *typical* mode whose relaxation time is comparable with t . We think this is the reason why we could obtain (18) using only the scaling property of single loop-excitation.

Although the network looks apparently quite complicated, a most simple characterization of it will be the following. The network structure consists of loops of various sizes which are hierarchically nested so that larger ones enclose smaller ones inside. (A similar picture was proposed before by Villain concerning the organization of *droplets* in spin-glass phase, see [13]). From this simple picture, the dynamics can be regarded as one of the hierarchical diffusion processes which have been intensively studied in rather abstract contexts, for example the *ultradiffusion* models [15]. It is interesting to note that in the latter models the autocorrelation function (return probability) shows asymptotically algebraic decay with some temperature dependent exponent, which is also the case in the dynamical overlap function in the present model. Furthermore, it has already been shown by Sibani and Hoffman that hierarchical diffusion processes can show aging effects [14]. Thus it will be fruitful to construct a phenomenological theory of the aging effect of the present model from this point of view. A study in this direction will be reported elsewhere [16].

Acknowledgement: The author would like to thank sincerely Prof. H. Takayama for valuable discussions and critical reading of the manuscript. He would also like to thank Dr. H. Reiger,

Prof. K. Nemoto, K. Hukusima and T. Komori for stimulating discussions. This work was supported by Grand-in-Aid for Scientific Research from the Ministry of Education, Science and Culture, Japan. The author was supported by Fellowships of the Japan Society for the Promotion of Science for Japanese Junior Scientists.

REFERENCES

- [1] For a recent review of DPRM and various related topics, see Halpin-Healy and Y.C. Zhang 1995, Phys. Rep. **254**.
- [2] D. S. Fisher and D. A. Huse 1988, Phys. Rev. **B 38** 373 and **B 38** 386.
- [3] D. S. Fisher and D. A. Huse 1991, Phys. Rev. **B 43** 10728.
- [4] T. Hwa and D.S. Fisher 1994, Phys. Rev. **B 49** 3136.
- [5] M. Mézard 1990, J. Phys. (France) **51**, 1831.
- [6] D. S. Fisher, M. P. A. Fisher and D. A. Huse 1991, Phys. Rev. **B43** 130.
- [7] Lundgren L., Svedlindh P., Nordblad P. and Beckmann O., Phys. Rev. Lett. 1983 **51** 911.
- [8] Refregier Ph., Vincent E., Hammann J. and Ocio M. 1987 , J. Phys. (Paris) **48** 1553.
- [9] Heiko Rieger 1993, J. Phys. **A 26**, L615.
- [10] J. O. Anderson, J. Mattson and D. Svedlindh 1992, Phys. Rev. **B46** 8297.
- [11] S. Franz and H. Rieger 1995, J. of. Stat. Phys. **79** 704.
- [12] J. P. Bouchaud 1992, J. Phys. (France) **2** 1705.
- [13] J. Villain 1986, EuroPhys. Lett. **2** 871.
- [14] P. Sibani and K. H. Hoffmann 1989, Phys. Rev. Lett. **63** 2853.
- [15] C. P. Bachas and B. A. Huberman 1987, J. Phys. **A20** 4995.
- [16] H. Yoshino, in preparation.

FIGURE CAPTIONS

Fig. 1: A representation of a configuration of 1+1 dim. RSOS DPRM.

Fig. 2: The three different cases a), b) and c) of the local configuration around a segment (see text for the definition). The possible new states 1, 2 and 3 of the segment are enclosed by boxes.

Fig. 3: The density plot of $P_\mu(z, x)$ (see text for definition) on a certain sample of random potential μ ($N = 100$, $T = 0.3$, $g = 0.01$ and $\sigma = 0.5$).

Fig. 4: A time sequence of $x(80)$ on the same system shown in Fig. 3. The positions of the four traps a, b, c and d are indicated.

Fig. 5: A schematic picture of a loop-excitation. The polymer (bold line) inside the left tube jumps over the void to the right tube and vice versa.

Fig. 6: The procedure of the temperature quench experiment.

Fig. 7: The waiting time t_w dependence of $q(t_w, t_w + t)$: $N = 300$, 10^2 samples at a) $T = 0.1$ and b) $T = 0.2$. The waiting time increases as $t_w = 2, 4, 8, \dots, 1024$ (MCS) from the bottom to the top curve.

Fig. 8: A scaling plot of the dynamical overlap function on the system of $N = 300$ and $T = 0.17$ by the scheme (14). The scale of the vertical axis is arbitrary. The dotted line represents the power law t^{-x} using x obtained by the fit (15). The solid line represents the power law $t^{-\lambda}$ with λ obtained by the direct fit of the $t/t_w \gg 1$ part.

Fig. 9: Double logarithmic plot of $C(t_w, T)$ v.s. t_w at $T = 0.17, 0.25, 0.30, 0.40$ and 0.50 . The scale of the vertical axis is arbitrary. The dashed lines are the fit by the algebraic law (15) with $x(T)$ presented in Fig. 10.

Fig. 10: Temperature dependence of the exponents : $\lambda(T)$ and $x(T)$. They are obtained

from data of ($N = 300, 10^2$ samples).

Fig. 11: Saturation of aging effect due to the finite size effect ($N = 20, T = 0.5, 500$ samples). q_{rep} was calculated by the transfer matrix method.

Fig. 12: FDT relation ($N = 20, T = 0.2, 10^4$ samples). The top three curves are the l.h.s. of (9) (correlation) of different waiting times $t_w = 40, 200$ and 1000 (MCS). The three curves below are the r.h.s of (9) (response) of corresponding t_w .

Fig. 13: Functional form of the response function ($N = 30, T = 0.20, 10^4$ samples and $N = 60, T = 0.40, 5 \times 10^3$ samples with $h = 0.03$). The solid line represents $\log(t)^2$ law (18).

Fig. 14: The density plot of $P(z, x)$ on a certain sample of small system at a high temperature. ($N = 20, T = 1.00$)

Fig. 15: The FDT relation (9) of a small system at a high temperature ($N = 20, T = 1.00, h = 0.1, 500$ samples) for $t_w = 4, 32, 256$ (MCS). The horizontal line is $h/T\chi_e$ where χ_e (see (12)) is obtained by transfer matrix method.

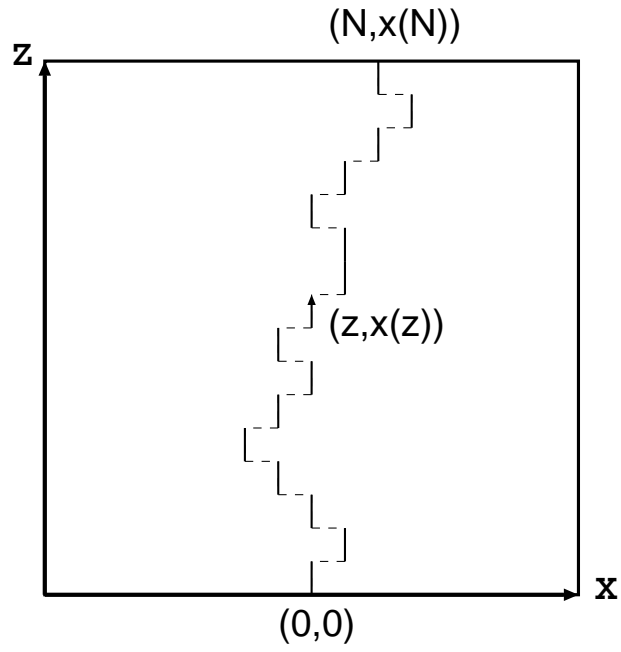


Fig. 1: A representation of a configuration of 1+1 dim. RSOS DPRM.

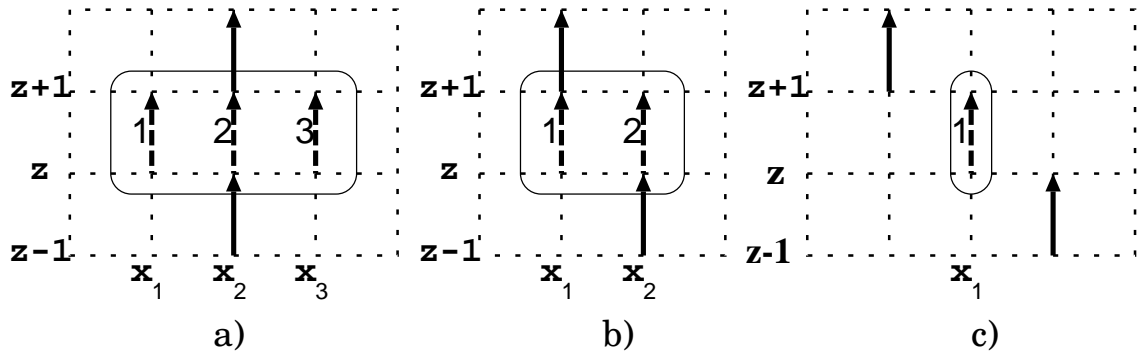


Fig. 2: The three different cases a), b) and c) of the local configuration around a segment (see text for the definition). The possible new states 1, 2 and 3 of the segment are enclosed by boxes.

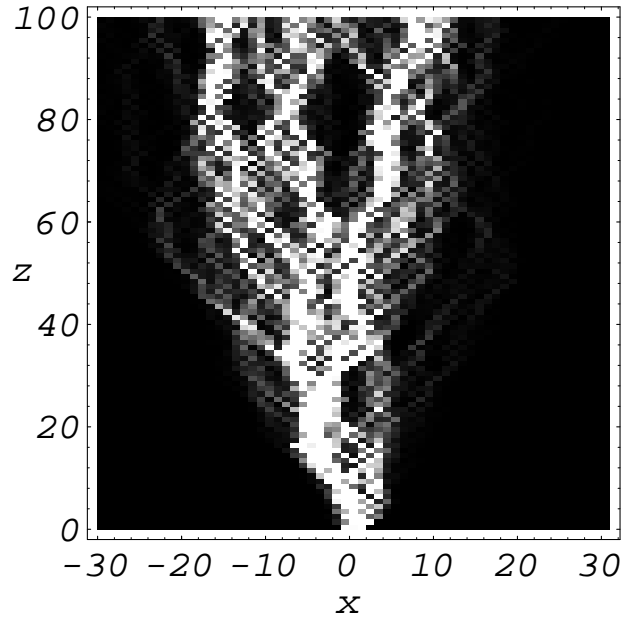


Fig. 3: The density plot of $P_\mu(z, x)$ (see text for definition) on a certain sample of random potential μ ($N = 100$, $T = 0.3$, $g = 0.01$ and $\sigma = 0.5$).

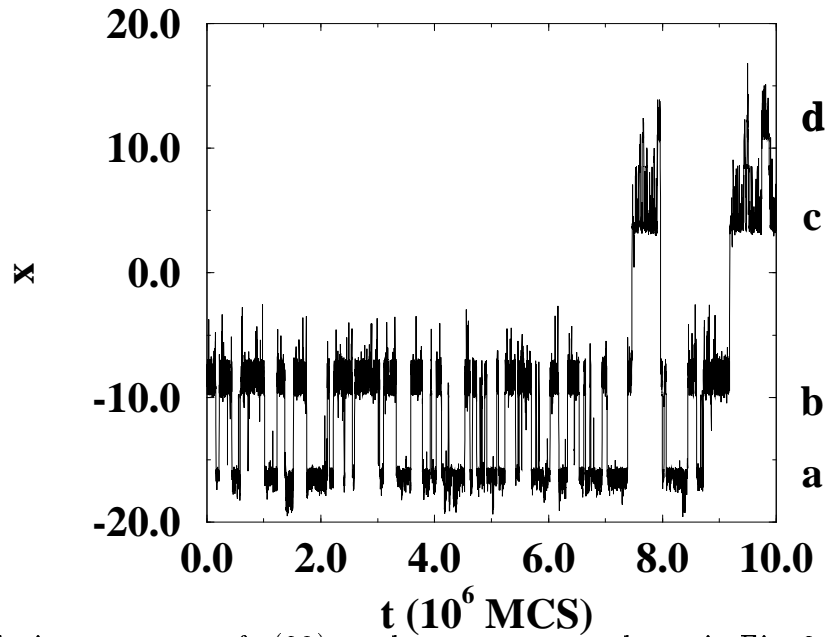


Fig. 4: A time sequence of $x(80)$ on the same system shown in Fig. 3. The positions of the four traps a, b, c and d are indicated on the right side.

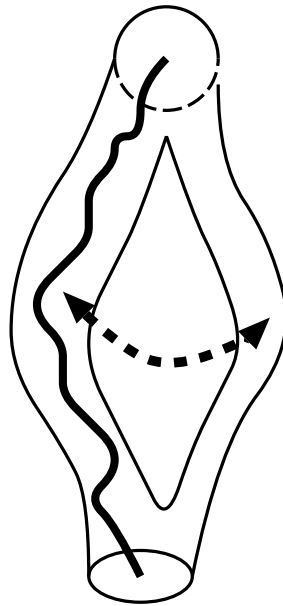


Fig. 5: A schematic picture of a loop-excitation. The polymer (bold line) inside the left tube jumps over the void to the right tube and vice versa.

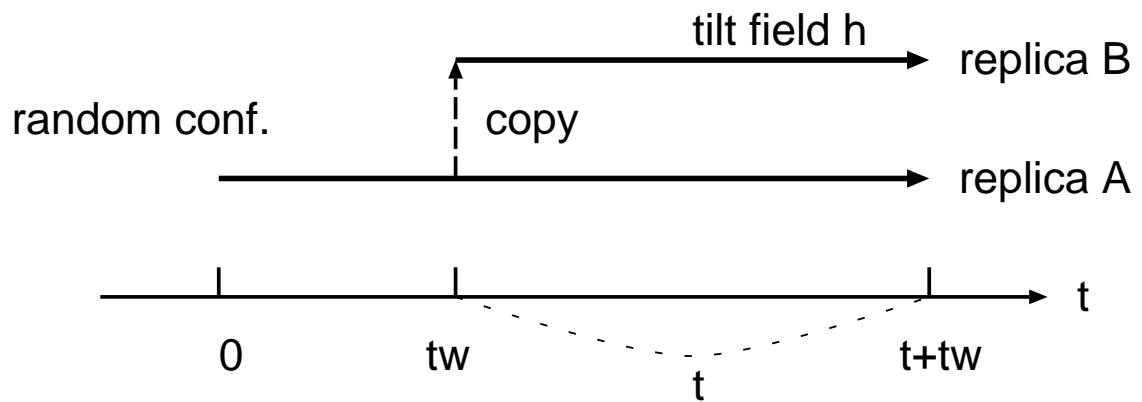


Fig. 6: The procedure of the temperature quench experiment.

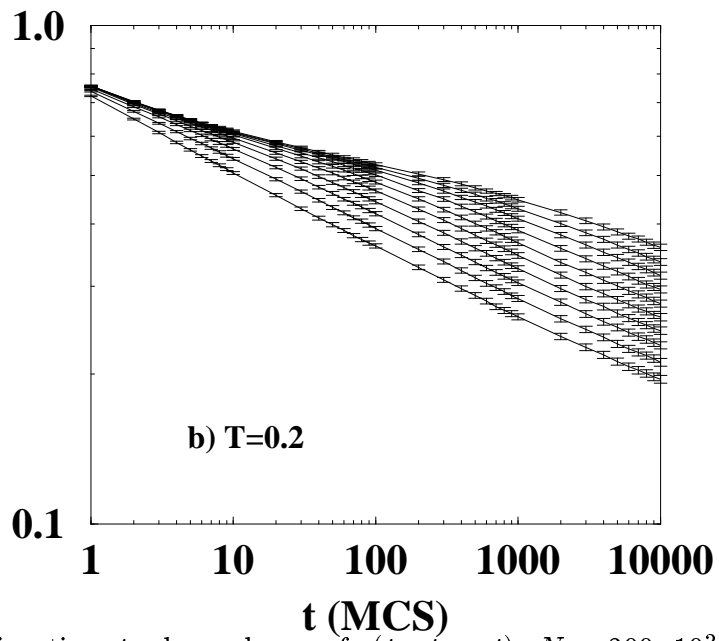
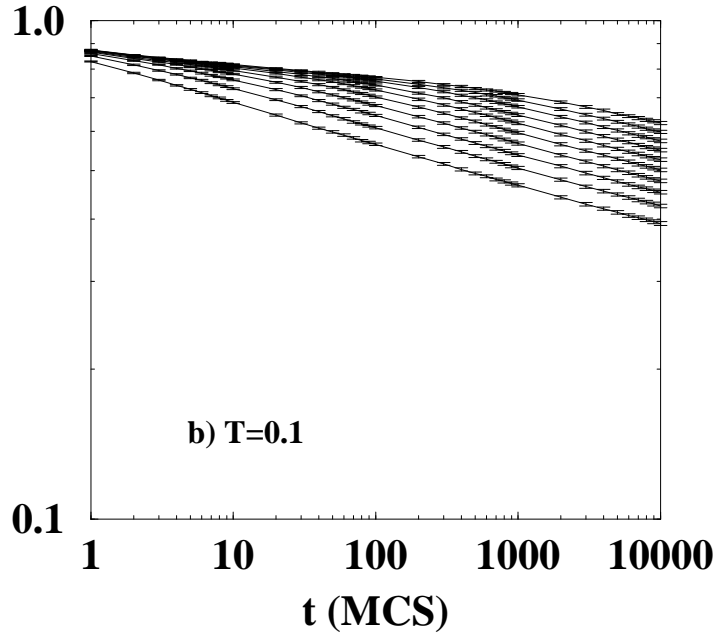


Fig. 7: The waiting time t_w dependence of $q(t_w, t_w + t)$: $N = 300$, 10^2 samples at a) $T = 0.1$ and b) $T = 0.2$. The waiting time increases as $t_w = 2, 4, 8, \dots, 1024$ (MCS) from the bottom to the top curve.

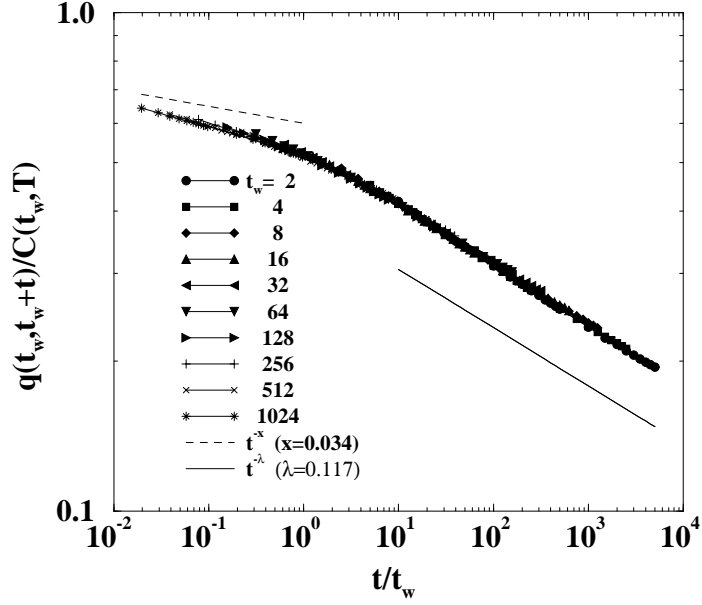


Fig. 8: A scaling plot of the dynamical overlap function on the system of $N = 300$ and $T = 0.17$ by the scheme (14). The scale of the vertical axis is arbitrary. The dotted line represents the power law t^{-x} using x obtained by the fit (15). The solid line represents the power law $t^{-\lambda}$ with λ obtained by the direct fit of the $t/t_w \gg 1$ part.

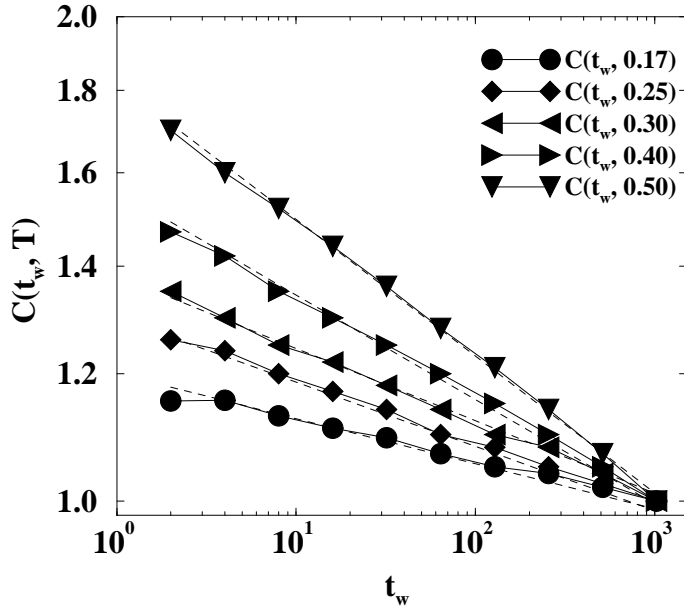


Fig. 9: Double logarithmic plot of $C(t_w, T)$ v.s. t_w at $T = 0.17, 0.25, 0.30, 0.40$ and 0.50 . The scale of the vertical axis is arbitrary. The dashed lines are the fit by the algebraic law (15) with $x(T)$ presented in Fig. 10.

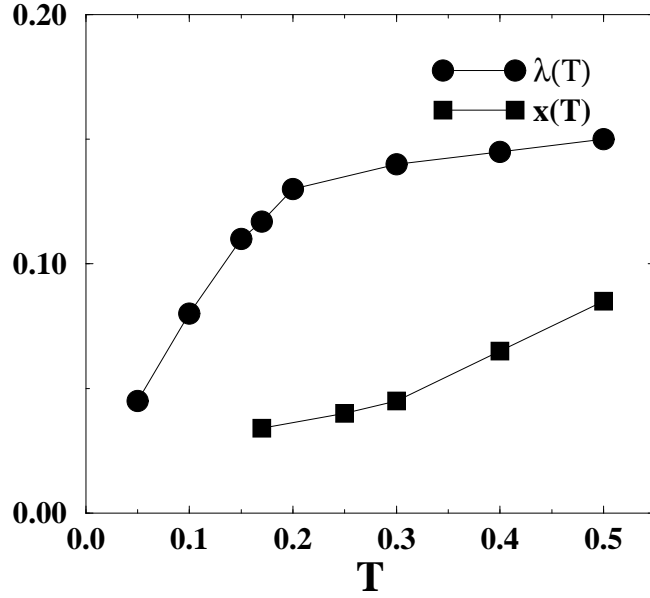


Fig. 10: Temperature dependence of the exponents: $\lambda(T)$ and $x(T)$. They are obtained from data of ($N = 300, 10^2$ samples).

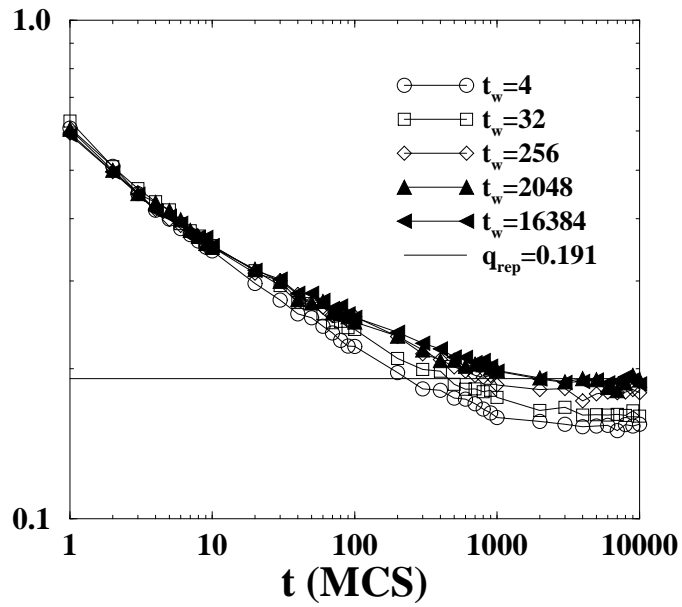


Fig. 11: Saturation of aging effect due to the finite size effect ($N = 20, T = 0.5, 500$ samples). q_{rep} was calculated by the transfer matrix method.

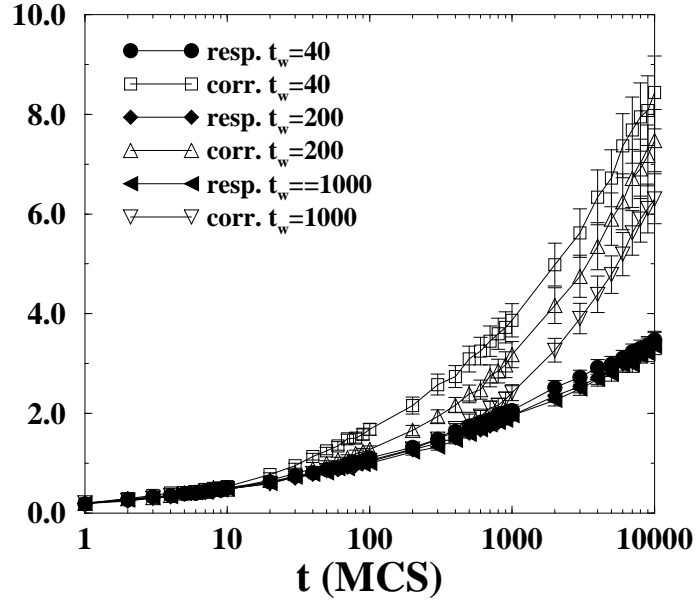


Fig. 12: FDT relation ($N = 20$ $T = 0.2$ 10⁴ samples). The top three curves are the l.h.s. of (9) (correlation) of different waiting times $t_w = 40, 200$ and 1000 (MCS). The three curves below are the r.h.s of (9) (response) of corresponding t_w .

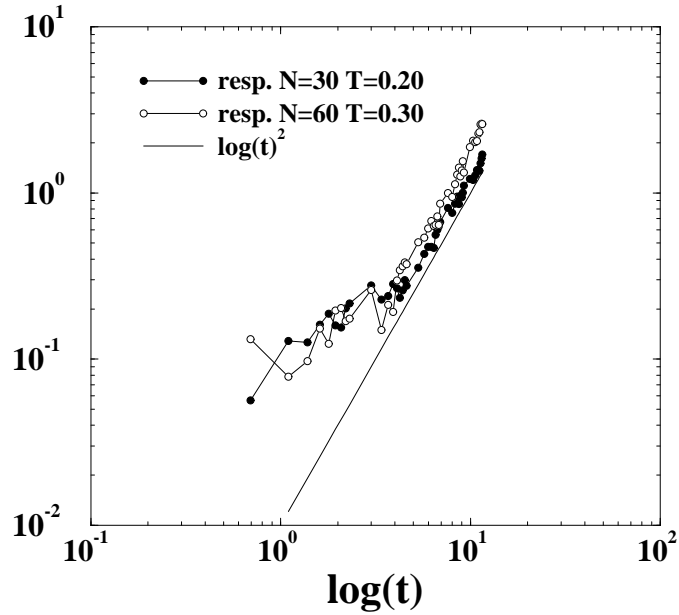


Fig. 13: Functional form of the response function ($N = 30$, $T = 0.20$, 10⁴ samples and $N = 60$, $T = 0.40$, 5 × 10³ samples with $h = 0.03$). The solid line represents $\log(t)^2$ law (18).

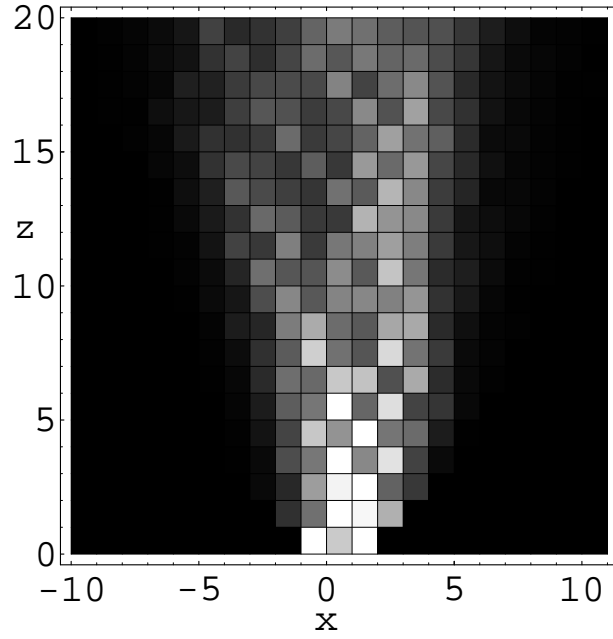


Fig. 14: The density plot of $P(z, x)$ on a certain sample of small system at a high temperature. ($N = 20$, $T = 1.00$)

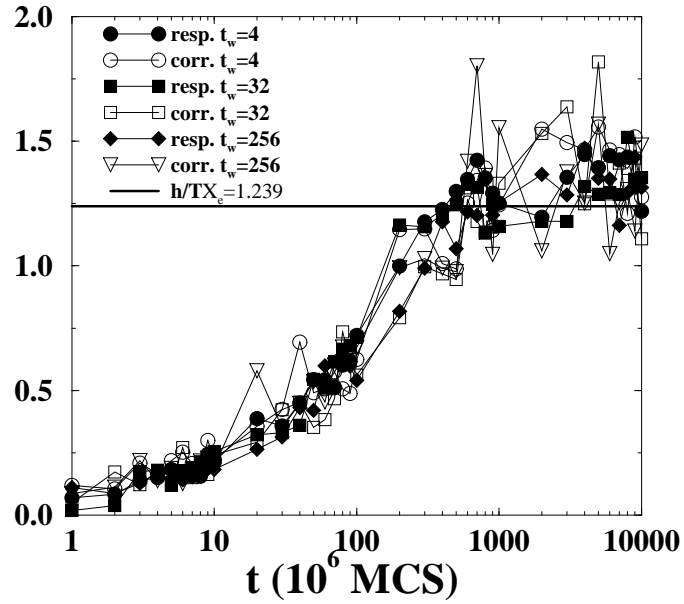


Fig. 15: The FDT relation (9) of a small system at a high temperature ($N = 20$, $T = 1.00$, $h = 0.1$, 500 samples) for $t_w = 4, 32, 256$ (MCS). The horizontal line is $h/T\chi_e$ where χ_e (see (12)) is obtained by transfer matrix method.